Hollow Cathode Discharge Initiation and Fast Starting Cathode

IEPC-2009-026

Presented at the 31st International Electric Propulsion Conference,
University of Michigan • Ann Arbor, Michigan • USA
September 20 – 24, 2009

Binyamin Rubin[1] and John D. Williams[2]
Department of Mechanical Engineering

Colorado State University

Fort Collins, CO 80523

Abstract: Conditioning of the insert inside a hollow cathode is believed to be important to ensure reliable discharge initiation and subsequent cathode operation. The desorption of contaminates is reported from hollow cathodes as a function of heater power to quantify cathode conditioning characteristics and identify factors that might prevent the fast initiation of a discharge. In addition to conditioning, a study of hollow cathode emission characteristics under no gas flow (i.e., vacuum) conditions was performed to judge the health of the insert and cathode surfaces. Results of these two studies are described herein along with measurements of the temperature of the cathode as a function of time and heater power. The data are used to validate a transient surface diffusion model that describes the migration and surface coverage fraction of low-work function material from the interior of the hollow cathode to the orifice barrel and to the exterior surface of the orifice plate of a conventional, orificed hollow cathode. A sufficiency condition is presented for our cathode geometry of vacuum emission current level and the ability to start a hollow cathode discharge once gas flow is initiated. Based on the results of the modeling effort and experimental validation campaign, a prototype fast-starting cathode with a directly heated insert design was fabricated. This configuration does not use a traditional hollow cathode tube with an orifice plate. Instead, the insert is simply supported by the coils of a swaged tantalum heater, which allows heat to be transferred directly from the heater to the insert. Therefore the insert heats up and starts to release low work function material faster than in the traditional configuration. More importantly the surface of the insert starts emitting electrons immediately once low work function material is released, while in a traditional hollow cathode the low work function material must first diffuse from the interior of the cathode to the surface of the orifice plate before electron emission becomes possible. Measurements of vacuum emission current on the fast starting cathode are presented that confirm the advantages described above.

Nomenclature

A	=	Richardson constant
E_τ	=	desorption activation energy
E_D	=	diffusion activation energy
e	=	electron charge

[1]Postdoctoral Researcher, Department of Mechanical Engineering, Colorado State University, brubin@engr.colostate.edu
[2]Assistant Professor, Department of Mechanical Engineering, Colorado State University, johnw@engr.colostate.edu

i = emission current
j = current density
k = Boltzmann's constant
M_{Ba} = mass of barium atom
P = barium partial pressure
R_{Ba} = radius of barium atom
r = radius from cathode centerline
T = temperature
V = voltage
φ = work function
θ = fractional surface coverage
τ = desorption time

I. Introduction

TO develop fast-starting cathodes necessary for example in short sounding rocket experiments or in collision avoidance situations where an electric propulsion device must be turned on and operated quickly, a better understanding of the cathode activation process is required[1]. Contaminates like H_2O, CO_2, O_2, ... can cause slower than desired ignition times or in extreme cases a total failure to start. We have measured desorption of contaminates as a function of heater power to quantify cathode conditioning characteristics. The conditioning study included measurements of cathode temperature and out-gassing using Line of Sight Residual Gas Analysis. We find that outgassing profiles from conventional planar cathodes are similar to those from our hollow cathode and orifice plate geometry, which is expected because both types of cathodes use similar inserts. A study of hollow cathode emission characteristics under vacuum conditions was also performed. We find that vacuum thermionic emission of electrons from the orifice plate at rates of ~15μA is adequate to ensure a cathode will start once gas flow is applied.[1] Consequently, the temporal behavior of emission from a hollow cathode is critically important in determining the time required to start a cathode. In cathodes that have degraded inserts due to long operation or exposure to contaminates, it is possible that the vacuum emission rate may never exceed ~15μA and, consequently, may not start when desired. In this sense, the model we present can be used to construct a life time model of a hollow cathode if the degradation of the insert's barium production processes can be quantified.

Measurements of current-voltage characteristics using a fast sweeping power supply are used to determine the effective work function of the cathode orifice plate surface as a function of time. Contrary to intuition, the work function increases with temperature at temperatures above 1000 ºC, which is in agreement with experiments on planar cathodes. The C-V temporal data are used to validate a transient surface diffusion model that describes the migration and surface coverage fraction of low-work function material that diffuses from the interior of the hollow cathode to the orifice barrel and to the exterior surface of the orifice plate of the cathode. Model fitting parameters are in close agreement with values found in the literature. Comparisons between the temporal behavior of the no-flow emission current and a model of this process show good agreement and demonstrate that a predictive model of cathode start time is now available.[1] The model can be used for optimizing hollow cathodes to reduce the ignition time as we show herein.

A prototype fast-starting cathode with an enclosed keeper was fabricated and tested. This configuration does not use a traditional hollow cathode tube with an orifice plate. Instead, the insert is simply supported by the coils of a swaged tantalum heater, which allows heat to be transferred directly from the heater to the insert. Therefore the insert heats up and starts to release low work function material faster than in the traditional configuration. More importantly the surface of the insert starts emitting electrons immediately once low work function material is released, while in a traditional hollow cathode the low work function material must diffuse from the interior of the cathode to the surface of the orifice plate before the electron emission becomes possible. Measurements of vacuum emission current and cathode start times are presented that confirm the advantages described above.

II. Experimental System

The experiments on hollow cathodes described herein are performed in a 0.3 m^3 stainless steel vacuum chamber pumped with a CTI Cryogenics On-Board 8 cryogenic pump (pumping speed 1500 liters/second for air). The pressure is monitored using a Varian 531 thermocouple gauge and a Varian 843 ionization gauge. The operating pressure during no-gas-flow cathode experiments is below $5x10^{-7}$ Torr. Fast starting cathode experiments were performed in the Veeco SPECTOR stainless steel vacuum chamber, which is similar to the chamber described above.

The cathode tip temperature was measured using type C thermocouples (tungsten+5% rhenium – tungsten+26% rhenium) spot welded to the orifice plate of the cathode. To reduce heat losses through the thermocouple wires, small diameter (0.075 mm) wires are used. To reduce measurement errors, small radiation shields made of tantalum are placed over the TC junctions. A Leybold TSP TR200 Residual Gas Analyzer (RGA) is used to measure partial pressures of

various gases during the cathode conditioning. The RGA is oriented so that gases flowing from the cathode orifice would be directed along the line of sight to the RGA entrance. A Kepco BOP 100-4 bipolar power supply/amplifier is used to bias the keeper relative to the cathode, which was connected to the vacuum facility ground. A Wavetek 114 function generator is used to control the power supply/amplifier during the fast voltage sweep measurements. For the fast starting cathode activation tests two TDK-Lambda ZUP power supplies were used for the heater and the anode, while a third TDK-Lambda ZUP was diode-summed in parallel with a high voltage Spellman SL1200 series power supply to power the keeper. A Brooks mass flow controller 5850e rated for 50 sccm Argon flow with a Brooks model 5896 power supply/readout are used to control xenon flow. An Agilent 34970a data acquisition/switch unit with a 34901a multiplexer card is used for voltage and temperature measurements. A PC with LabView is used to perform data logging tasks.

III. Cathode Conditioning and Activation Study

A. Measurement of Outgassing During Cathode Conditioning

As mentioned above, before a hollow cathode discharge can be initiated, it is necessary to prepare the cathode for operation. This process is called conditioning and can take tens to hundreds of minutes for some cathodes. The purpose of conditioning is the safe removal of contaminants like water, oxygen, carbon dioxide, etc. from the low-work function insert located within the hollow cathode tube near its downstream (orificed) end. The process of safely removing contaminant gases is achieved by slowly increasing the cathode temperature with increasing heater power while the cathode is held in a pristine vacuum environment. The slow ramping of temperature is necessary because the porous tungsten insert may be "poisoned" by the out-gassing contaminants if the cathode is heated too quickly[2]. By "poisoned" we mean that non-reversible chemical reactions would be induced within the matrix of the insert and on its surface that would result in a permanent and unacceptably high work function. The pristine vacuum environment is necessary to prevent chemical reactions from occurring at high rates on the surface of the insert, which can occur in poor vacuum environments containing high concentrations of water vapor, oxygen, and carbon dioxide. The following conditioning sequence is used. First, the heater current is set to 2 A and then increased by 1 A every 5 minutes until a level of 6 A is reached. At this point, the heater current step size is reduced to 0.5 A, and two additional steps of 5-minute duration are performed at 6.5 and 7.0 A. It is noted that conditioning can be performed with or without gas flow through the cathode, and, typically, we perform the conditioning process without gas flow. A conditioning sequence of heater current and subsequent heater voltage is shown in Fig. 1. Note that different cathode configurations and heater designs are used in practice resulting in (1) different heater current, voltage, and power characteristics and (2) different conditioning sequences. The temperature during conditioning is shown in Fig. 2. Note that because low (~20 ºC) temperatures are outside of the C-type thermocouple measurement range, the initial temperatures indicated for all curves are incorrect, and correspond not to zero degrees Celsius, but to room temperature (~20 ºC).

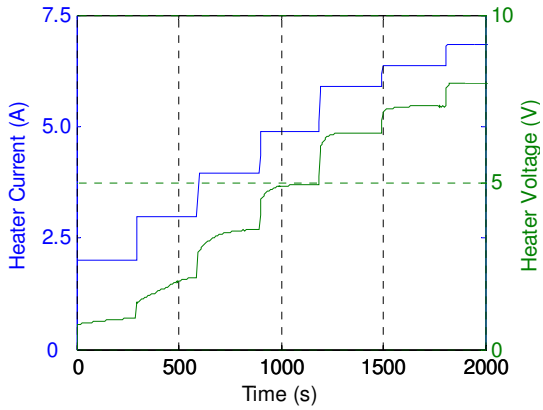

Figure 1. Hollow cathode conditioning: heater current and voltage vs. time.

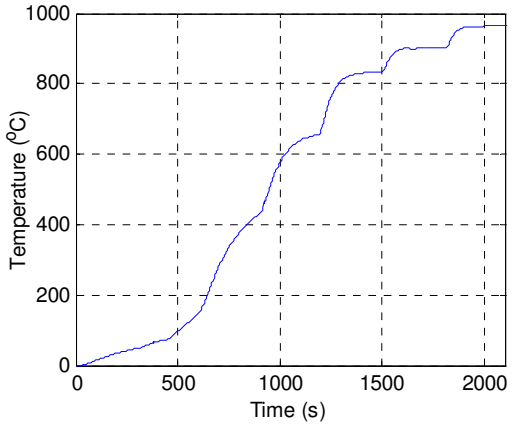

Figure 2. Hollow cathode conditioning: orifice plate temperature vs. time.

During conditioning of the cathode, outgassing was monitored using a technique known as Line of Sight Residual Gas Analysis (LOSRGA)[3]. Desorption of water, carbon dioxide and atomic oxygen (the latter most probably being a daughter ion of water) as a function of time are shown in Fig. 3 (using the same time scale of Figs. 1 and 2). The most significant desorption occurs between 700-900 ºC. Haas observed desorption of these three components at slightly lower temperatures for M cathodes[4]. It is interesting to note, however, that Haas also observed a single major peak for water and multiple peaks for carbon dioxide as we see in this study.

B. Emission current measurements and work function calculation

After conditioning is performed, the hollow cathode can be started (i.e., a plasma discharge can be established between the keeper electrode and cathode). The minimum requirements to start the cathode include (1) temperature of approximately 1100 ºC; (2) gas flow in the range of 1-10 sccm; and (3) a keeper potential bias, usually in the range of 50V to 200V. A final requirement for starting orificed cathodes with small orifice diameters is for the insert to coat the hollow cathode interior, orifice barrel and orifice plate exterior with a partial mono-layer of barium oxide. To check the condition of a cathode at a given point in its use history, the cathode heater is turned on (usually at a nominal level of 7 A) when the cathode is initially at room temperature and the vacuum emission current from the cathode orifice plate is monitored versus time.

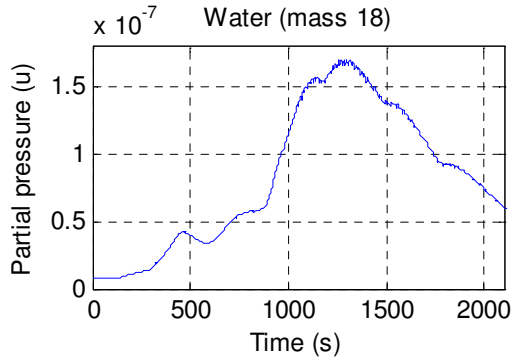

a)

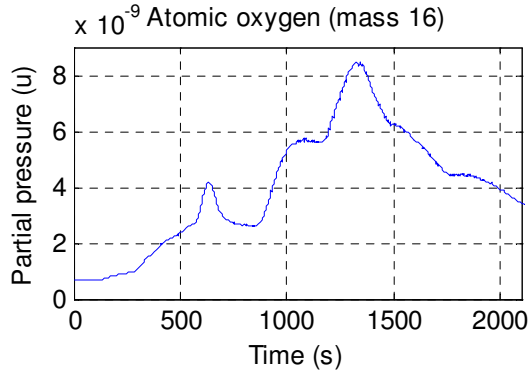

b)

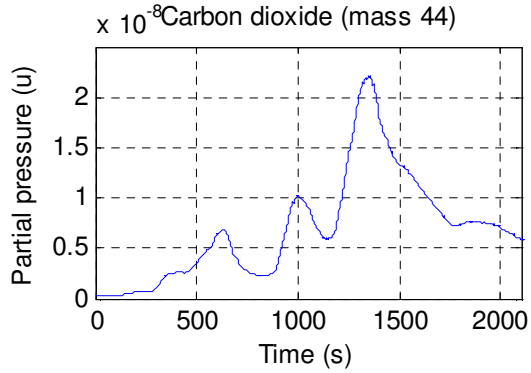

c)

Figure 3. Desorption of gases during conditioning.

Vacuum emission current measurements were performed herein using a fast sweeping power supply to bias the cathode relative to an electron collecting electrode (i.e., the keeper electrode described earlier). Measurements were made of the emission current versus bias voltage while the cathode was heated (from room temperature to its final operating temperature) with the gas flow off. The bias waveform was created by injecting a triangularly shaped waveform with amplitude of 1 V from a function generator into the Kepco BOP 4-100 power supply that amplifies the 1V amplitude signal to 110 V in amplitude. The frequency of the waveform generator signal was set to 0.5 Hz. Since we are only interested in positive voltages and snapshots of the I-V data versus time, we only used one-half of the bias waveform (i.e., the section of the bias waveform as it rose from about 0 V to +100V over a period of about 0.5 seconds during which the temperature of the orifice plate was approximately constant). The heater voltage and power values corresponding to the applied heater current levels are given in Table 1. Note that these voltage and power values were reached after the cathode was heated to thermal equilibrium.

As expected, higher heater power levels cause emission to start sooner and reach higher saturation values. The saturation value is dependent upon both the cathode temperature and the surface coverage fraction of barium oxide on the exterior of the cathode orifice plate. The low-voltage section of the I-V curve displays emission that is space-charge limited corresponding to the Child-Langmuir law. At higher voltages, emission is temperature-limited.

Measured current-voltage characteristics were used to determine an effective work function of the orifice plate surface using the technique described by Burtner[5] and Tonnere et al.[6] Briefly, the high-voltage part of each current-voltage characteristic corresponding to the voltage region from 90 V to 100 V, where the emission is temperature-limited, as opposed to space charge limited emission at lower voltage, was extrapolated to zero voltage on a Schottky plot to obtain the zero-electric-field saturated current density. Note that the surface-averaged current density was obtained by dividing the emission current by the orifice plate area. The Richardson-Dushman equation was then used to calculate the effective work function of the orifice plate:

$$\varphi = -\frac{kT}{e}\log\left(\frac{j}{AT^2}\right), \qquad (1)$$

where k is the Boltzmann constant, e is the electron charge, T is the temperature, j is the zero-field current density, and A is Richardson's constant. The results are presented in Fig. 4 for three different heater current levels. Note that during the first 3 minutes of heating the emission current is below the sensitivity limit of our measurement system, and the work function could not be determined.

Table 1. Heater current, voltage and power values

Heater current (A)	Steady-state heater voltage (V)	Steady-state heater power (W)
6.0	7.0	42.0
7.0	8.8	61.6
7.5	9.6	72.0

In all cases the work function initially drops as the temperature increases from ~850ºC to 950ºC, reaches a minimum at a temperature near 1000ºC, and then increases with time and orifice plate temperature. The increase of the work function with temperature seems unreasonable at first. This is because the rate of barium release from the insert increases at elevated temperatures, which would imply increased barium surface coverage and a reduction in work function. The unreasonableness of the results shown in Fig. 4 can be resolved by considering the rate of barium evaporation from the cathode surface relative to its supply rate. As the temperature increases, the lifetime of a barium atom on the surface of tungsten decreases. As a result, the barium surface concentration can drop when the evaporation rate exceeds the supply rate, and one will observe an increase of the effective work function. Reduction of barium surface concentration with an increasing temperature for planar surfaces was analyzed by Thomas[7], and increases in work function with temperature on planar cathodes were observed experimentally by Rittner[8].

The voltage range of the sweeping power supply was limited to approximately 110 V and so additional measurements were carried out over an extended voltage range of 0-300V to ensure temperature-limited emission conditions were present. These higher voltage range I-V characteristics of the cathode were measured at steady-state conditions. To achieve steady state emission behavior the cathode was held at a given temperature until no further change was observed in the emission current measured at a fixed keeper bias of ~300 V. The time to reach steady-state emission was several hours.

Effective work function dependence on cathode temperature for steady-state measurements is presented in Fig. 5. These values were based on data collected between 290 V and 300 V that were extrapolated to zero field on a Schottky plot. It is noted that work function drops with increasing temperature, reaching a minimum at 1036 ºC, and then increases with increasing temperature. This result is in reasonable agreement with the temporal data presented where a minimum was observed at about 900-1000 ºC.

Steady-state current-voltage characteristics were also used to estimate the error in work function values determined during temporal cathode heating experiments performed with a sweeping keeper voltage, which were performed over a smaller range of voltages. Specifically, the zero-field saturated emission current and work function values were determined from the steady state I-V data sets using data between 90 V and 100 V and data between 290 and 300 V. The results of the calculations, presented on Fig. 5, show that the maximum error in effective work function is about 0.15 eV between the two voltage ranges. Our steady state measurement system was limited to 300 V, and no measurements at higher voltages were performed. Use of higher voltages would allow one to determine work functions more accurately, however, from the shape of the current-voltage curves and the agreement between the 100 V and 300 V data sets, we conclude that the effective work function does not differ significantly from the work function determined using the 300 V data.

For low temperatures between 800-900 ºC the differences in work function are very low, but for temperatures 1000 ºC and above the differences are more significant. To understand the discrepancy between the two curves, it should be noted that different regions of the orifice plate surface have different work function. At any given bias condition, some regions of the orifice will emit electrons in space-charge limited mode, described by Child-Langmuir law, others – in saturated (temperature-limited) mode, described by the Richardson-Dushman equation. The emission current measured in our experiment is a total current emitted from the entire orifice plate surface. The effective work function, calculated from this current, is an area averaged value, that is used to characterize a work function of the entire surface. At minimum voltage, emission is space charge limited for the entire surface. As the keeper voltage increases, parts of the surface with progressively lower work function become saturated. If the effective work function is high, saturated emission (i.e., temperature-limited) conditions will exist over most of the orifice plate surface. On the other hand, a lower effective work function would require higher voltages to ensure temperature-limited emission. Therefore, for an orifice plate with only a small region at a low work function condition, even a small 100 V bias is enough to saturate almost the entire surface, and obtain a reasonable estimation of the effective work function value.

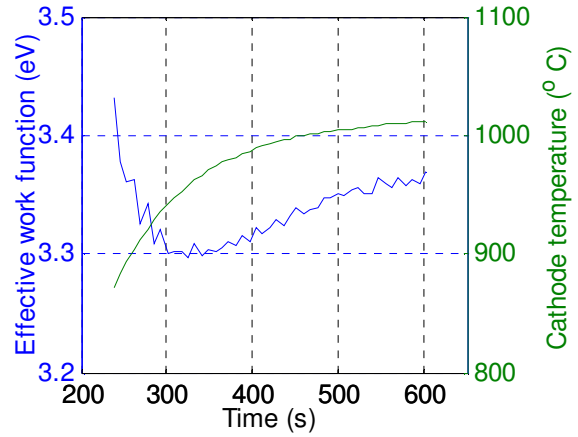

(a)

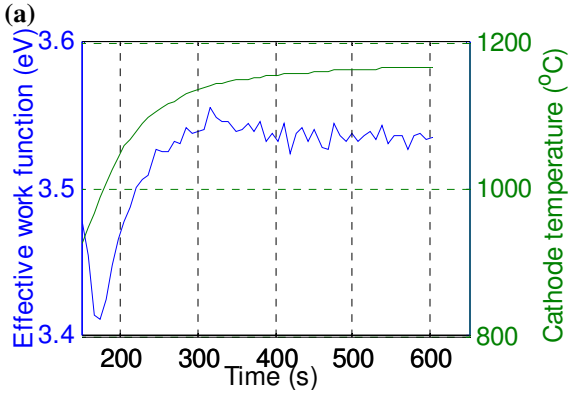

(b)

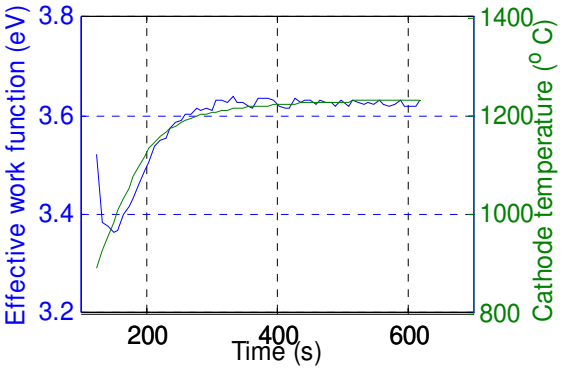

(c)

Figure 4. Effective work function and cathode temperature vs. time heater current: (a) 6A, (b) 7A, (c) 7.5 A.

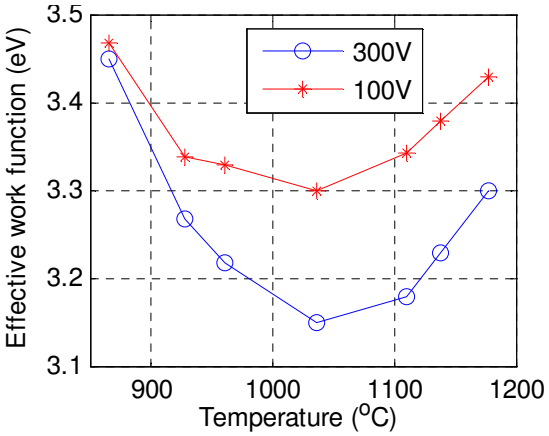

Figure 5. Effective work function at cathode orifice plate vs. temperature; star - calculated from low-voltage part of current-voltage curve (90-100 V) , open circle – from full range (290-300 V).

C. Cathode discharge ignition

Cathode activation tests were conducted using another cathode, that has the same dimensions as the cathode used in the outgassing and emission study. Two types of hollow cathode ignition tests were performed. During the first test, the heater was turned on at 7 A and a keeper bias of 50 V was applied. When the emission reached a pre-selected value, a flow of xenon gas at 5 sccm was turned 'on'. If the cathode didn't start, the flow was turned 'off' and then turned back 'on' at a (pre-selected) higher vacuum emission level. These experiments showed that a minimum, no-flow emission current value of 15 μA ±3 μA was necessary to start the cathode, which is in good agreement with the value of 21μA ±10 μA reported by Tighe[9]. During the second test, the heater current, keeper bias, and flow were turned 'on' simultaneously and the emission current was recorded until the cathode discharge ignited. These experiments demonstrated that with a gas flow of 5 sccm, the emission current starts to increase earlier and increases more rapidly. As a result, the cathode can be started in less time. The relationship between emission current temporal behavior under no-flow conditions and with gas flow is beyond the scope of this paper, but is believed to be important especially for cathodes that need to be started quickly in experiments that need to be conducted during limited duration tests. The results of the ignition tests are presented in Fig. 6.

Although further investigation would be needed to account for the effect of gas flow on discharge initiation, there are several explanations that might be proposed. The first is improved transport of barium to the interior of the orifice plate due to xenon flow. Our estimation shows that the flux of barium toward the orifice plate due to xenon flow is about one hundredth of the thermal flow of barium that is present both with and without the xenon flow. This is because the xenon axial drift velocity is approximately 100 times lower than the barium thermal velocity. Therefore any barium carried by xenon flow cannot significantly increase the surface coverage on the orifice plate, and, in turn, increase the emission current. A second explanation is higher ionization rates in the ignition region of the cathode due to higher xenon pressure, as suggested by Tighe[9]. This option also seems to be less likely, because before ignition, the emission current is very low. A third explanation is improved surface diffusion on the interior of the cathode due to higher surface coverage gradients. Without xenon, the barium pressure in the cathode is very low, and the mean free path of barium atoms is much larger than the diameter of the cathode. With xenon flow, the mean free path of barium atoms is estimated to be on the order of 0.1 mm. Therefore the return rate of barium atoms to the surface is greater with xenon present than without, leading to higher local surface coverage of the interior surfaces. Higher surface coverage will lead to higher surface gradients and higher surface diffusion rates to the orifice plate, which in turn will enhance emission.

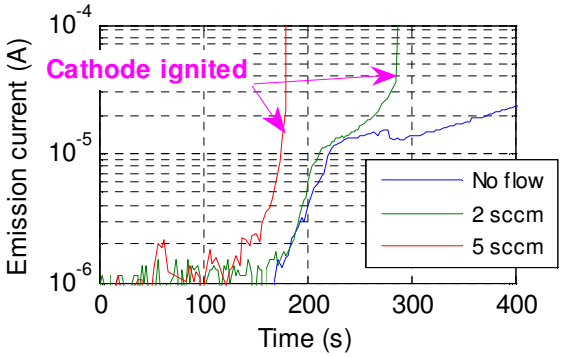

Figure 6. Results of cathode activation tests.

IV. Cathode Emission Model

As described above, the cathode start-up sequence begins with applying power to the heater that causes the cathode temperature to increase, eventually reaching approximately 1100 ºC. As the cathode heats up, barium evaporates from the cathode insert, creating a barium gas, which fills the inside of the cathode tube. Eventually, a coating of barium covers the inner surfaces of the hollow cathode and the orifice plate. To determine barium surface coverage of the inner surfaces, including the orifice barrel walls we use the following continuity equation[10-14]

$$\frac{\partial \theta_0}{\partial t} = k_a(1-\theta_0) - \frac{\theta_0^{\,p}}{\tau}\,, \tag{2}$$

where θ_0 is the surface coverage fraction of the inner surfaces, limited by a monolayer[13-15] that corresponds to $\theta_0 = 1$; t is time; k_a is a parameter proportional to the barium pressure inside the cathode; and τ is the desorption time of barium atoms. The first term on the right side reflects the fact that the rate of adsorption on a surface being considered is proportional to the ratio of uncovered-to-total area[14], the second term describes desorption of barium adatoms from the surface [11,13,15]. The parameter p in Eq. (1) is a constant, it compensates for the concentration dependence of the desorption time. Rittner[8] suggests that the value of this parameter is between 4 and 5, and justifies this range theoretically based on repulsion between adatoms. The value of p=5 represents a best fit to experimental data of Forman[15] and is used herein. Although p=5 is a conventionally accepted value, Free and Gibson [12] noticed that the value of 8 represents a better fit to their data, while Longo[14] used a value of 1, explaining that the interaction between barium atoms on the surface is most effective near a monolayer.

The value of k_a in Eq. (2) is[13]:

$$k_a = 2R_{Ba}^2 P\sqrt{\frac{\beta}{M_{Ba}}}, \tag{3}$$

where R_{Ba} is the radius of a barium atom; $\beta = 1/kT$, *with* k as the Boltzmann constant and T as the orifice plate temperature; M_{Ba} is the mass of a barium atom; and P is the barium partial pressure inside the cathode[9,16]:

$$P = P_0 \exp\left(\frac{\varepsilon_p}{T}\right), \tag{4}$$

where P_0 and ε_p are empirical constants. The parameter P_0 can be modified to include pressure reduction that can occur during the cathode aging[9,14] or when poisoning gases are present, but these processes are not considered here. The porous tungsten insert used in our experiments was new, and therefore no correction for the age of the insert was required. The desorption time τ is calculated from

$$\tau = \tau_0 \exp\left(\beta E_\tau\right), \tag{5}$$

where τ_0 is an empirical constant and E_τ is the desorption activation energy.

Assuming that the time required to reach equilibrium surface coverage on the cathode inner surfaces is much lower than the characteristic time of surface diffusion[9,10], discussed below, we obtain:

$$k_a(1-\theta_0) = \frac{\theta_0^5}{\tau}. \tag{6}$$

Solving this nonlinear equation for θ_0 provides the surface coverage fraction on the orifice barrel walls, which is used as a boundary condition for the surface diffusion equation, described below.

The barium deposited on the interior surface of the orifice plate and within the orifice barrel diffuses to the outer surface of the orifice plate, creating a low work function emitter. This process is described by another continuity equation, describing the surface diffusion and desorption of barium atoms [9-11]:

$$\frac{\partial\theta}{\partial t} = D\nabla^2\theta - \frac{\theta^5}{\tau}, \tag{7}$$

where θ is the surface coverage fraction of the outer orifice plate surface and D represents the surface diffusion coefficient:

$$D = D_0 \exp\left(-\beta E_D\right), \tag{8}$$

where D_0 is an empirical constant and E_D is the activation energy for diffusion.

Using r as the radius from cathode centerline, the boundary conditions for the surface diffusion equation are:

$$\theta = \theta_0(t),\ r = r_1; \quad \theta = 0, \quad r = \infty, \tag{9}$$

where θ_0 is the surface coverage of the orifice barrel walls (r=r_1), determined from Eq. (5). The outer boundary of the solution domain was placed further from the orifice than the actual outer orifice plate boundary. This condition does not restrict the surface coverage on the outer boundary of the orifice plate, but instead reflects the fact that barium can diffuse from the orifice plate to the outer walls of the cathode. Values of τ_0 and E_τ were determined by fitting the model to experimental data, as described below.

After the surface coverage is determined, the work function φ over the exterior of the orifice plate can be determined using the equation derived by Longo[14]:

$$\varphi(\theta) = \varphi_W \left(\frac{\Gamma \varphi_W}{\varphi_{Ba}} \right)^{\frac{\Gamma\theta}{1-\Gamma}} + \varphi_{Ba} \left[1 - \left(\frac{\Gamma \varphi_W}{\varphi_{Ba}} \right)^{\frac{\theta}{1-\Gamma}} \right]. \quad (10)$$

In Eq. (10), Γ represents the parameter that determines the minimum work function at monolayer coverage determined from Longo's data[14] φ_W the tungsten work function and φ_{Ba} the barium work function.

Now we calculate the emission current density j using the Richardson-Dushman equation combined with the Schottky term:

$$j = AT^2 \exp\left(-\beta\varphi(\theta) + \beta \sqrt{\frac{e^3}{4\pi\varepsilon_0}} \sqrt{\frac{V}{d}} \right), \quad (11)$$

where A is Richardson's constant, e is electron charge, ε_0 is vacuum permittivity, V the bias voltage between the cathode and the keeper electrode, and d the distance between the cathode and the keeper electrode. This equation describes the field-enhanced, thermal emission from the exterior surface of the orifice plate. The experimental measurements, described above, were performed using fast voltage sweeps with a maximum voltage of approximately 100 V. Time dependent current values corresponding to 100 volts were used to minimize the influence of space charge emission, that was not included in the model. Considering the relatively low current densities obtained in experiments, the effect of space charge is negligible. Integrating the current density over the orifice plate surface we obtain the emission current:

$$i = 2\pi \int_{r_1}^{r_2} j(\varphi) r dr \,. \quad (12)$$

The emission current behavior is estimated using the experimentally measured orifice plate temperature. A thermal model was also developed and validated, and either temperatures calculated from the thermal model or ones directly measured result in identical behavior.

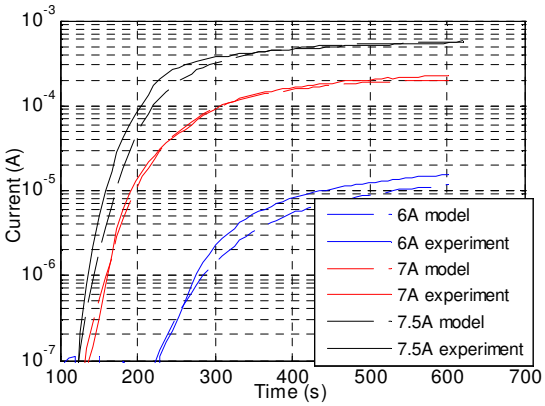

Figure 7. Model best fit to experimental emission current

The values of parameters P_0, ε_p, E_τ, D_0, E_D were determined using a least squares fit to experimental data. The value of τ_0 =2.13*10^{6}s^{-1} was used, following Jensen[13] and Forman[15]. The fitting was performed using the emission data for all heater currents (6A, 7A, 7.5A) with the same set of parameters. A large-scale, trust-region, reflective Newton algorithm available in MATLAB was used to perform the fitting calculations. For parameter ε_p, the best fit value is -18538 K, which is close to -21960 K, determined by Rittner et al.[16]. The best fit value for the desorption activation energy E_τ is 2.05 eV, which is practically identical to the value of 2.06 eV, determined by Forman[15]. The best fit for diffusion activation energy E_D is 0.6918 eV, which is close to the value 0.73 eV, determined by Rittner[11] but is lower than the value of 1.4 eV reported by Thomas[10].

The emission current profiles obtained by fitting the model to the experimentally measured emission current, as well as the experimental data, are presented in Fig. 7, where reasonable agreement is observed over the three heater power levels investigated. Therefore it can be concluded that physically meaningful values of parameters P_0, ε_p, E_τ, D_0, and E_D were obtained.

The model can be used for optimizing hollow cathodes to reduce the ignition time. One important conclusion from these results is that surface diffusion plays a significant role in the cathode activation, since low work function material released from the insert must diffuse onto the surface of the orifice plate before the cathode can be activated.

V. Fast starting cathode

A prototype fast-starting cathode with enclosed keeper was fabricated based on the results of the research described in Section IV. A simple sketch of the fast-starting cathode is shown in Fig. 8 where a swaged tantalum heater is directly coiled around a porous tungsten insert impregnated with a mixture of barium calcium aluminate and scandate. A Swagelok tee is used to direct gas flow to the insert and pass the coaxial heater lead to a location where a gas tight electrical power connection can be made. Radiation shielding made from 10 layers of 0.013 mm thick tantalum foil wrapped around the heater was used to increase heater efficiency. An enclosed keeper electrode made from a stainless steel tube with a tantalum orifice plate was placed over the insert-heater assembly. The keeper is biased positive relative to the cathode to initiate a plasma discharge directly between the insert and keeper.

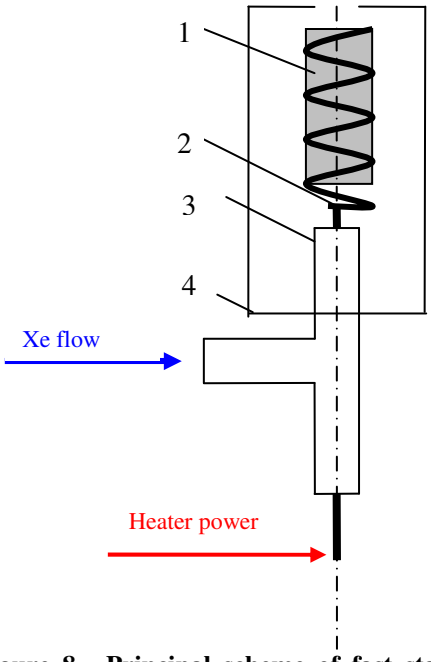

Figure 8. Principal scheme of fast starting hollow cathode. *1-insert, 2 – heater with radiation shield, 3 - Swagelok tee, 4 – keeper electrode.*

The directly heated insert configuration does not use a traditional hollow cathode tube with an orifice plate and an external heater that requires one to transfer heat from the heater through the tube to the insert. Therefore the insert heats up and starts to release low work function material faster compared to traditional configurations. Another advantage of the directly heated insert design is that the surface of the insert itself serves as the low work function emitter instead of the orifice plate of a traditional cathode design (see Section IV). The surface of the directly heated insert starts emitting electrons once low work function material is released, while in a traditional hollow cathode design, the low work function material must diffuse onto the surface of the orifice plate before electron emission becomes possible. The heater for the directly heated insert cathode was fabricated in-house using coaxial tantalum heater wire insulated with magnesium oxide. The porous tungsten insert was fabricated by Spectra-Mat Inc. using type 532-x impregnate, which is an air stable mixture of barium calcium aluminate that is supplemented with scandate at 4-8%. In this mixture, the scandate additive serves as a catalyst for barium and barium oxide production for regions of the impregnate that are not in direct contact with the surfaces of tungsten pores.

Measurements of vacuum emission current are presented that confirm the advantages described above. During typical measurements the keeper electrode was biased 50V relative to the cathode. Figure 9 compares emission profiles of the fast-starting cathode compared and a regular hollow cathode. Both measurements were performed with new inserts that had never been activated before and had only been conditioned once. The emission of the fast-starting cathode begins to increase sooner and grows much faster compared to the emission from a traditional cathode. Emission levels reach 15 μA (indicative of starting time) in about 3 minutes.

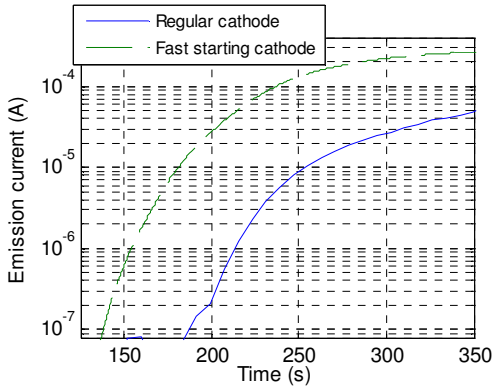

Figure 9. Comparision of emission profiles.

A series of cathode ignition tests were performed to evaluate the directly heated insert design. During the tests the keeper electrode was biased at a positive voltage relative to the cathode, xenon flow was turned on, and then the heater was turned on. After the heater was activated, the emission current was monitored as a function of time. The time from the heater activation to the cathode discharge ignition was measured for different operating conditions. To activate the discharge rapidly, it is necessary to build up xenon pressure of several Torr inside a cathode. In a traditional hollow cathode, the cathode tube and orifice plate serve this purpose, and either enclosed or open, toroidal-based keeper configurations can be used. In the prototype fast-starting cathode, an enclosed keeper-keeper orifice plate design is necessary. Although early experiments confirmed that the discharge in the new cathode configuration can be activated even without the enclosed keeper, much longer starting times (~600 sec) were required.

Cathode starting tests were performed with different xenon flow rate and keeper bias. The objective of the tests was to determine if an optimum keeper voltage and xenon flow rate combination exists that would facilitate rapid initiation of the cathode discharge. The electrical diagram of the test setup is shown in Fig. 10. Two power supplies were used for the keeper bias, one high-voltage and one low-voltage, that were diode summed together. The high voltage power supply allowed keeper bias voltages as high as 900 V to be investigated, but it had limited current capability, therefore the second power supply capable of providing several amperes of current at low voltage was added. During most of the starting tests described herein, the anode was biased 100V relative to the cathode; and the current to the keeper was limited to 1 A while the current to the anode was limited to 3.6 A. The cathode was connected to ground via a 1 Ohm

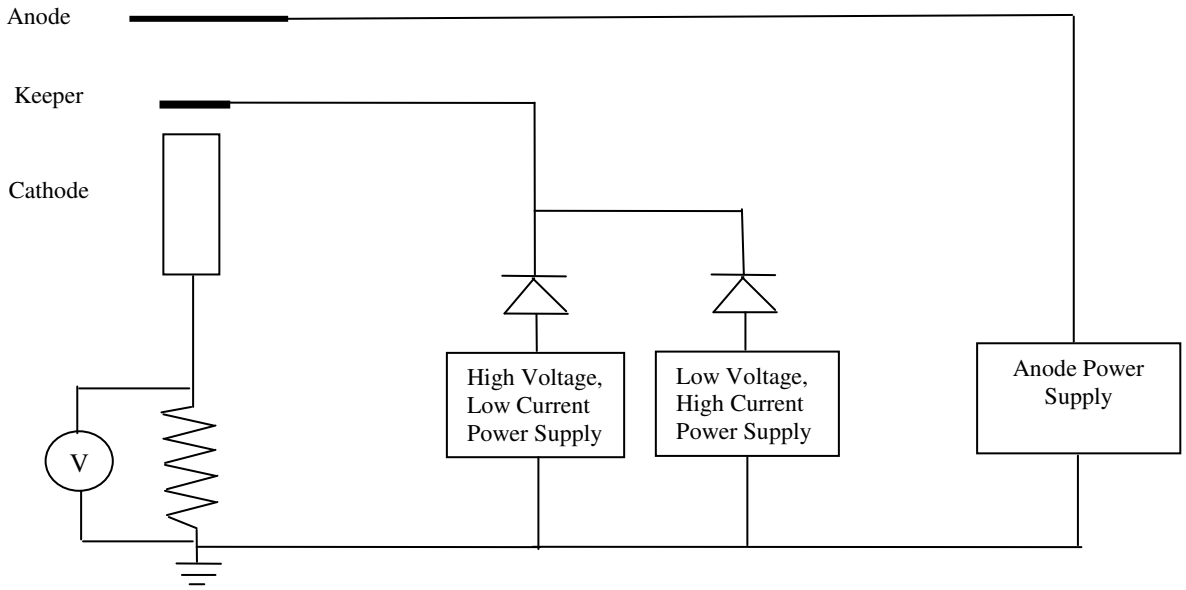

Figure 10. Electrical circuit used during activation tests.

shunt and the voltage induced across the shunt was used to calculate the cathode emission current.

Ignition tests were performed with two different keeper orifice diameters – 0.04" and 0.08" to check the influence of the orifice diameter on cathode activation time. Although experiments suggested that the orifice diameter affects starting time, the starting time was observed to increase by only 20 sec +10 sec when the orifice size was increased from 0.04" to 0.08". The larger keeper orifices, however, was found to facilitate a much lower voltage discharge between the cathode plasma and the anode, and this feature is especially important for a plasma contactor cathode that must be able to couple easily to space plasma environments. Since the difference of the starting time for the two orifice diameters investigated was not very significant, the larger orifice size is preferable. We note that future work could be performed to optimize the keeper orifice geometry.

An example of cathode emission measured during a starting test is presented in Fig. 11. The current, plotted on logarithmic scale, increases as the cathode heats up, once the cathode discharge starts, the current quickly rises to a maximum value limited by the power supply setting. From the data in Fig. 11, the activation time was determined to be 116 s for a flow rate of 10 sccm and keeper bias of 200 V, 120 s for 15 sccm flow and 900 V, and 132 s for 30 sccm and 200 V.

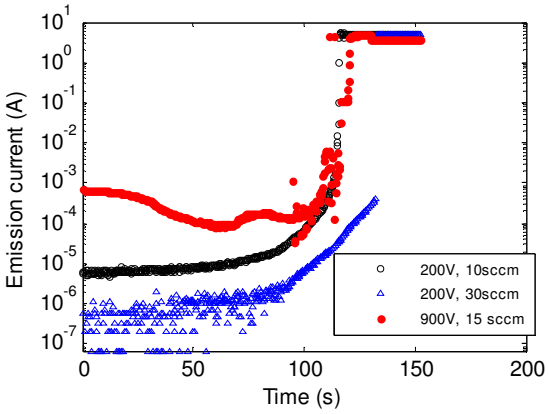

Figure 11. Fast starting hollow cathode emission current.

Many tests similar to the ones shown in Fig. 11 were performed over xenon flow rates from 2 to 50 sccm and keeper biases from 50 to 900 V. After each cathode ignition event, the discharge, keeper, and heater power supplies were turned off and the cathode was allowed to cool down for 1 hour. The results of the tests are presented in Table 2. Most of the tests were repeated several times, and, for these tests, the average of several activation times is given in the table. The results of the experiments demonstrate that an increase of mass flow rate above 10 sccm does not reduce starting time. Although start times are slightly longer at lower flow rates, it was also observed that the fast starting cathode design resulted in very noisy and unstable discharges at flows below 6 sccm. Therefore, the optimal range of mass flow rates that allows fast starts with a stable discharge is 6 to 10 sccm for the geometry of our cathode.

At mass flow rates less than 15 sccm plume mode discharges were observed as shown in Fig. 12a. At a mass flow rate above 30 sccm the discharge was more spot mode-like in appearance as shown in Fig. 12b. The discharge was observed to switch between plume and spot mode at flow rates between 15 and 30 sccm.

Results presented in Table 2 also show that keeper bias above 200 volts does not improve starting time. Therefore we conclude that optimal conditions to activate this cathode design are 6-10 sccm xenon mass flow rate and 100-200 V keeper bias.

In addition to tests where DC keeper biases were used, some tests were performed with pulsed keeper biases. In these tests the same electrical circuit shown in Fig. 10 was employed with the low voltage power supply set at 50 VDC for all tests. The high voltage DC power supply was replaced by a custom-built power supply fabricated by Colorado Power Electronics, Inc. This power supply can be switched on and off very fast, which allows one to obtain pulse durations on the order of microseconds. During one set of tests, the pulse amplitude was set to 700 V with a duration of about 5 ms, during another set of tests, the amplitude was set to 300 V with a duration of 20 μs. For both sets of tests, the pulse repetition frequency was fixed at ~50 Hz. The results indicated that the cathode activation time does not improve with high voltage pulsing.

Some differences in starting times were detected when a cathode was left off for more than 12 hours. Specifically, the time necessary to activate the cathode for the first time after a long idle period was 20-25 seconds longer than the time at the same conditions, but after only one hour from the previous activation. This is most probably caused by the gradual (and reversible) poisoning of the insert by residual gases. It is noted in this regard that the baseline pressure was 1.3×10^{-6} Torr. Reactive gases, such as oxygen, water vapor, carbon dioxide, make up a significant fraction of the residual vacuum atmosphere under base pressure conditions, and exposure to partial pressures of reactive gases as low as 3×10^{-8} Torr are known to poison a barium-oxide-based cathode[1,3]. After the cathode is heated, it recovers within tens of seconds.

To check the possibility of starting a cathode without conditioning after atmospheric exposure, as required for a sounding rocket mission, the following experiment was carried out. The cathode was first exposed to atmosphere for more than 12 hours. Next the vacuum chamber, in which the cathode was mounted, was pumped down to high vacuum (2.4×10^{-6} Torr), and the cathode was purged with 10 sccm Xe flow for 5 minutes. Next the heater current was ramped from zero to the nominal 4 A level over 1 minute, after which the nominal heater current was maintained until the cathode discharge ignited. A xenon flow rate of 10 sccm and a keeper bias of 200 V were used in this test. The resulting cathode activation time was 152 seconds. After the test the cathode was allowed to cool down to the room temperature, and a health check was performed, i.e. the emission current profile at 200 V keeper bias without gas flow was measured as a function of time after applying the nominal heater current. The health check demonstrated that no significant poisoning occurred to the insert as a result of the fast ignition experiment described above. We conclude from this preliminary test that the fast starting cathode design described herein can be activated without prior conditioning as required during sounding rocket missions.

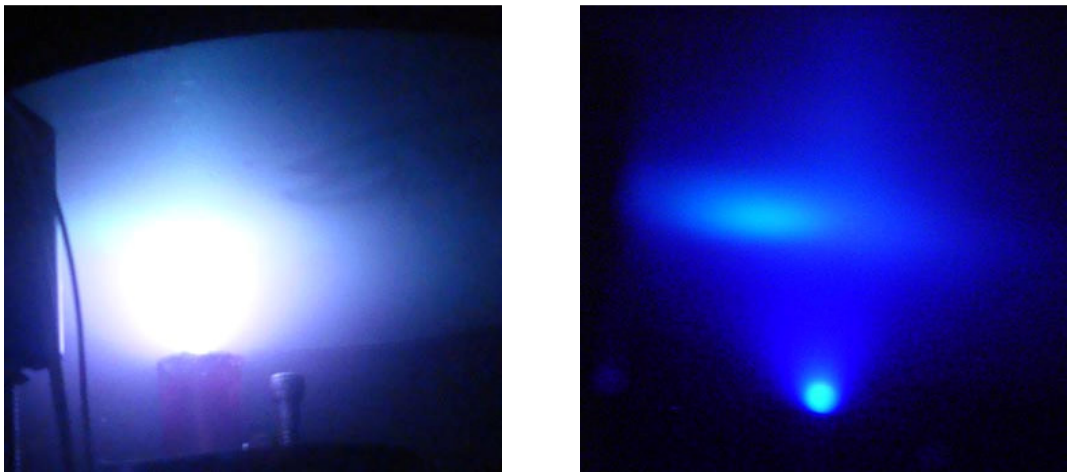

a **b**

Figure 12. Hollow cathode discharge in plume mode (a) and in spot mode (b).

TABLE 2 **Cathode activation time vs. xenon mass flow rate and keeper bias.**

	V_k	50	100	200	300	600	900
$\dot{m}(Xe)$							
2				117			
5				125			
10		125	120	120.5	118	120	100
15		130.5	122	116.5	123	122	120
20			122.5	120	113	124	
30			120	132	130	109	
40				122			
50							

VI. Conclusion

Herein we present data on electron emission characteristics of hollow cathode devices equipped with barium containing compounds that are designed to be both conditioned and started in short times (i.e., in less than 3 minutes) using xenon flow rates of less than 10 sccm and applied voltages of less than 100 V. A model of the hollow cathode starting process based on surface diffusion of barium and barium oxide is presented and results are compared to experimental measurements under no-flow conditions. In general, good agreement is obtained between model and experiment suggesting that the important physics have been incorporated into the model. Relatively high gas flow rates of ~5 sccm and higher applied at the beginning of a start sequence are observed to shorten starting times significantly, and, consequently, the effect of gas flow warrants further study. A fast starting hollow cathode design was developed and fabricated during this study and preliminary data on starting time were collected. This cathode was started in less than 150 sec without being conditioning before starting as would be required on a sounding rocket mission. Subsequent vacuum emission (no flow) testing showed that the cathode was not damaged by the direct start operation. We conclude that it is possible to utilize direct starting hollow cathodes based on barium oxide inserts for sounding rocket missions or other applications that require fast starting capability.

Acknowledgments

The authors would like to thank Mr. Les Johnson, NASA Marshall Space Flight Center for partially supporting this work under grant NNM06AA25G.

References

[1]B.Rubin and J.D. Williams, "Hollow Cathode Conditioning and Discharge Initiation", *Journal of Applied Physics,* vol.104, 053302, 2008.

[2]J.E. Polk, "The Effect of Reactive Gases on Hollow Cathode Operation", 42nd AIAA/ASME/SAE/ASEE Joint Propulsion Conference & Exhibit, 2006, AIAA paper 2006-5153.

[3]B.C. Lamartine, W.V. Lampert, and T.W. Haas, "AES-RGA Investigation of Various Types of Cathodes During Activation in Ultrahigh Vacuum", Applied Surface Science, 171 (1981).

[4]G.A. Haas, R.E. Thomas, C.R.K. Marrian, and A. Smith, "Rapid Turn-On of Shelf-Stored Tubes: An Update", IEEE Transactions on Electron Devices, 38, 2244 (1991).

[5]D. Burtner, "Plasma contacting with a solid expellant" PhD Dissertation, Colorado State University (1999).

[6]J J.C. Tonnere, D. Brion, P. Palluel, and A.M. Shroff, "Evaluation of Work Function Distribution of Impregnated Cathodes", Applied Surface Science, 16, 238 (1983).

[7]R.E. Thomas, "Diffusion and Desorption of Barium and Oxygen on Tungsten Dispenser Cathode Surfaces", Applied Surface Science, 24, 538 (1985).

[8]E.S. Rittner, R.H. Ahlert, and W.C. Rutledge, "Studies on the Mechanism of Operation of the L-acthode. I", Journal of Applied Physics, 28, 156 (1957).

[9]W.G. Tighe, K. Chien, D.M. Goebel, and R.T. Longo, "Hollow Cathode Emission and Ignition Studies at L-3 ETI", Proceedings of the 30-th International Electric Propulsion Conference, Florence, Italy, September 17-20, 2007, IEPC-2007-023.

[10]R.E. Thomas, "Diffusion and Desorption of Barium and Oxygen on Tungsten Dispenser Cathode Surfaces", Applied Surface Science, 24, 538 (1985).

[11]E.S. Rittner, R.H. Ahlert, and W.C. Rutledge, "Studies on the Mechanism of Operation of the L-acthode. I", Journal of Applied Physics, 28, 156 (1957).

[12]B.A. Free, and R.G. Gibson, "Dependence of Surface Coverage on Pore Geometry in Dispenser Cathodes", Applied Surface Science, 24, .358, (1985).

[13]K.L. Jensen, Y.Y. Lau, and B. Levush, "Migration and Escape of Barium Atoms in a Thermionic Cathode," IEEE Transactions on Plasma Science, 29, 772 (2000).

[14]R.T. Longo, "Physics of Thermionic Dispenser Cathode Aging", Journal of Applied Physics, 94, 6966 (2003).

[15]R. Forman, "Surface Studies of Barium and Barium Oxide on Tungsten and its Application to Understanding the Mechanism of Operation of an Impregnated Tungsten Cathode", Journal of Applied Physics, 47, 5272 (1976).

[16]E.S. Rittner, W.C. Rutledge, and R.H. Ahlert, "On the Mechanism of Operation of the Barium Aluminate Impregnated Cathode", Journal of Applied Physics, 28, 1468 (1957).